Desalination and Water Treatment
www.deswater.com
doi: 10.1080/19443994.2013.811121

52 (2014) 6145–6155
September

Taylor & Francis
Taylor & Francis Group

Biosorption of methyl orange from aqueous solutions using cationic surfactant-modified wheat straw in batch mode

Yinyin Su, Yubin Jiao, Chanchan Dou, Runping Han*

School of Chemistry and Molecular Engineering, Zhengzhou University, No. 100 of Kexue Road, Zhengzhou 450001, PR China
Tel. +86 371 67781757; Fax: +86 371 67781556; email: rphan67@zzu.edu.cn

Received 19 April 2013; Accepted 22 May 2013

ABSTRACT

In this paper, the characterization of wheat straw (WS) and cetyl trimethyl ammonium bromide (CTAB) modified wheat straw (MWS) was determined by Fourier transform infrared spectroscopy (FTIR) and X-ray fluorescence (XRF), indicating that CTAB had entered into the structure of WS successfully. Then, MWS was used as adsorbent for the removal of methyl orange dye (MO, anionic dye) from aqueous solution in batch mode. The experiments were carried out by exploring the most suitable conditions including solution pH, MWS dosage, dye initial concentration, temperature, and contact time. Biosorption capacity of MWS for MO is 50.4 mg g^{-1} at 303 K under the optimum condition of pH of 3, MWS dosage of 1.00 g L^{-1}, contact time of 520 min. The Freundlich and Temkin models were all successful in depicting the equilibrium. The kinetic process can be predicted well by the Elovich, pseudo-second-order and intraparticle diffusion model. In addition, the thermodynamics parameters indicated the biosorption process was spontaneous and exothermal. The best desorption method for MO-loaded MWS was hot water. The results implied that MWS be suitable as effective adsorbent material for the biosorption of MO from aqueous solution.

Keywords: Biosorption; Modified wheat straw; Methyl orange

1. Introduction

In recent years, with the development of textile-printing technology, some new nonbiodegradation organics make chemical oxygen demand (COD) of textile printing up to 2,000–3,000 mg L^{-1}, which poses a huge challenge for traditional wastewater treatment means, such as flotation, coagulation. The dyestuff mainly comes from textiles, paper, leather, coating, and plastics [1]. Discharge of small amounts of dye effluent into natural rivers can lead to lower water clarity and seriously affect survival of aquatic life. Aromatic rings in dye structure form them carcinogenicity, inertia, and mutagenicity [2]. Thus, it is essential to remove dyes from effluents. In practice, many methods, such as oxidization and ozonation [3,4], electrochemical technique [5], adsorption, have been used to treat the wastewater containing dyes. Much attention has been paid on adsorption owing to its proven efficiency [6].

The activated carbon with large surface area is effective and widely used as adsorbent [7], but its cost is quite high. Therefore, many researchers pay attention to different types of low-cost materials from

*Corresponding author.

agricultural by-products, such as wheat or rice husk, De-oiled Soya, peanut husk, wheat straw (WS), and so on [8–22]. WS has an abundant source in north region of China and it is reported that annual production can be more than 600 million [23]. WS is mainly treated by burning or being abandoned. So researchers have interested in removing the dye in aqueous solution with WS, which not only can make full use of WS but also provide a novel method for dye effluent treatment [24]. As a major agricultural waste, WS has been investigated for utilizing in many studies. Usually, in order to improve the adsorbent capacity for the removal of dye, different modified methods are always used to improve the adsorbent capacity [12,25].

Natural wheat straw (NWS) has been used as an available adsorbent to remove heavy metals and dyes from water/wastewater [16,26]. But the capacity about anionic dyes was very low. Several researchers used cationic surfactant to modify agricultural byproduct to remove anionic ions pollutants [27–30]. But few investigations have been reported using WS modified by surfactants for dyes biosorption.

In the present study, cetyl trimethyl ammonium bromide (CTAB), one cationic surfactant, was used to modify NWS and enhanced its capacity toward anionic pollutants. Methyl orange (MO, C.I. 13,025, molecule weight 327.36 g mol^{-1}, CAS 547-58-0) is one of the well-known acidic/anionic dyes, and it has been widely used in textile, printing, paper, food, and pharmaceutical industries and research laboratories. Its structure is shown in Fig 1. Azo dyes are well-known carcinogenic organic substances. Like many other dyes of its class, MO on inadvertently enter the body through ingestion, metabolizes into aromatic amines by intestinal microorganisms [31]. In this study, MO was selected as objective to evaluate the capacity of modified wheat straw (MWS) toward anionic dyes.

This present work is aimed to study the biosorption properties through the effects of several factors on biosorption capacity. These factors include adsorbent dosage, pH value, temperature, initial concentration, and salt concentration. Adsorption models were selected to fit the experimental data as well as the thermodynamic parameters were calculated. Of course, the regeneration of MO-loaded MWS was also performed.

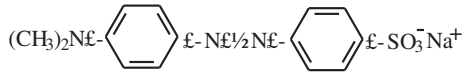

Fig. 1. Structure of methyl orange.

2. Materials and methods

2.1. Adsorbent preparation and characterization

Wheat straw (NWS) was obtained from local countryside, Zhengzhou City, China. The certain dosage straw was immerged into tap water for 24 h and then was dried in an oven at 330 K until constant weight. The straw materials were ground and screened through a set of sieves to obtain average size of 40−60 mesh and named as NWS. Five grams NWS was treated in 200 ml of 1% CTAB at room temperature for 24 h in constant oscillator. Then, the straw was washed thoroughly with deionized water until neutralized and dried in the oven at 333 K until constant weight. Finally, the resulting adsorbent named by MWS was stored in airtight container for further use to biosorption experiments.

The major elements of NWS and MWS were measured using elemental analyzer (MOD. 1,106, USA). Elemental compositions were obtained by X-ray fluorescence (XRF) spectrometer (Philips PW 2,404 X-ray fluorescence, the Netherlands). Fourier transform infrared (FTIR) analysis was used to study the surface functional groups, using FTIR spectroscope (PE-1710), where the wavelength was scanned from 4,000 to 400 cm^{-1} with a resolution of 4 cm^{-1}.

2.2. Dye solution

Stock solution of MO was prepared by dissolving 1.0 g of MO in 1 L distilled water, respectively. All working solutions were prepared by diluting the stock solution with distilled water to the desired concentration.

2.3. Biosorption studies

Effect of adsorbent dosage on the amount of MO removal was performed with different dose in a series of 20 ml 30 mg L^{-1} MO for 10 h, respectively, under the condition of pH 4.00 and 303 K.

To investigate the effect of initial solution pH on biosorption performance, experiments were carried out at constant dye solution (30 mg L^{-1}) and MWS dosage (1.00 g L^{-1}) with different initial pH from 2.00 to 12.00 at 303 K.

For the study of salt effect, adjust pH of MO to 3.00, and the rest of condition as same as above. The experiments were carried out with the NaCl and $CaCl_2$, varying the salt concentrations from 0.00 to 0.20 mol L^{-1}.

The concentration of dye was estimated by monitoring the absorbance changes at a wavelength of maximum absorbance (480 nm, Uv/Vis-3,000). The

equilibrium concentration in solid phase was calculated by the following expressions:

$$q_e = \frac{(C_0 - C_e)v}{m} \quad (1)$$

$$p = \frac{C_0 - C_e}{C_0} \times 100\% \quad (2)$$

where q_e is the biosorption amount of MO per gram MWS at equilibrium ($mg\,g^{-1}$), p is the percent removal efficiency (%), C_0, C_e are the concentration of dye at original and equilibrium ($mg\,L^{-1}$), respectively. v is the volume of solution (L), and m is the amount of MWS (g).

2.4. Equilibrium studies

Equilibrium studies were performed by using the suitable dosage of MWS with dye solution different initial concentrations. Batch Erlenmeyer flasks were shaken at a constant speed in the oscillator with the temperature 303, 313, and 323 K, respectively. After 10 h, these solutions were filtrated, and then the filtrate was analyzed at its maximum absorbance wavelength.

The equilibrium sorption isotherms are fundamental in describing the interactive behavior between adsorbates and adsorbent and are essential in giving an idea of the biosorption capacity of the adsorbent.

2.4.1. Langmuir Isotherm model

The Langmuir isotherm is the most popular isotherm model and it is mainly applied to describe the monolayer biosorption process. The corresponding mathematical expression is equation as follows [32]:

$$q_e = \frac{q_m K_L C_e}{1 + K_L C_e} \quad (3)$$

where q_m is the maximum amount of biosorption ($mg\,g^{-1}$), K_L is the biosorption constant ($L\,mg^{-1}$), q_e is sorption capacity at equilibrium ($mg\,g^{-1}$), C_e is equilibrium concentration of adsorbate ($mg\,L^{-1}$).

2.4.2. Freundlich isotherm model

The Freundlich model is a semi-empirical equation describing heterogeneous surface sorption and multilayer sorption under various nonideal conditions. This isotherm is commonly presented as [32]:

$$q_e = K_F C_e^{1/n} \quad (4)$$

where K_F is a constant representing the biosorption capacity, and $1/n$ is a constant depicting the biosorption intensity. K_F and $1/n$ are constants incorporating all factors affecting the biosorption process (biosorption capacity and intensity of biosorption).

2.4.3. Temkin isotherm model

The energy state which the Temkin isotherm may discribe is that the heat of biosorption fall with linear down with the biosorption capacity increasing. The Temkin model is expressed as [32]:

$$q_e = A + B \ln C_e \quad (5)$$

A, B are the Temkin constants.

2.5. Kinetic studies

In kinetic studies, the samples were collected at different time intervals and the experiments were carried out at 303, 313, and 323 K in a constant temperature. The residual concentration of MO was measured.

For further interpretation of biosorption behaviors, four common kinetic biosorption models (pseudo-first-order kinetic model, pseudo-second-order kinetic model, Elovich and intraparticle diffusion) were tested to obtain the rate constants and equilibrium biosorption capacity at different temperatures. For the pseudo-first-order kinetic model, it is assumed that biosorption rate is proportional to the difference between q_e and q_t [33]. The pseudo-second-order equation was based on the sorption capacity of the solid phase, and it is also considered that the biosorption process is controlled by a chemical sorption mechanism involving electron sharing or electron transfer between adsorbent and adsorbate [34]. The Elovich equation is used to describe the process where the activation energy has a great change [35]. In addition, the intraparticle diffusion model fits to describe the dynamic diffusion process which mainly exists in internal diffusion [29]. Thus, four equations are presented in the following:

Pseudo-first-order kinetic model:

$$q_t = q_e(1 - e^{-k_1 t}) \quad (6)$$

Pseudo-second-order kinetic model:

$$q_t = \frac{k_2 q_e^2 t}{1 + k_2 q_e t} \quad (7)$$

Elovich equation:

$$q_t = \frac{1}{\beta}\ln(a\beta) + \frac{1}{\beta}\ln t \quad (8)$$

Intraparticle diffusion equation:

$$q_t = K_t t^{1/2} + C \quad (9)$$

where q_t is biosorption quantity ($mg\,g^{-1}$) at time t, q_e is biosorption capacity at equilibrium ($mg\,g^{-1}$); k_1 is kinetic rate constant (min^{-1}), k_2 is pseudo-second kinetic rate constant ($mg\,g^{-1}\,min^{-1}$), K_t is diffusion rate constant ($mg\,g^{-1}\,min^{-0.5}$); C is constant ($mg\,g^{-1}$); a is the initial biosorption rate ($mg\,g^{-1}\,min^{-1}$); β is the constant relating to fraction of the surface covered and chemisorption activation energy($g\,mg^{-1}$).

All parameters of adsorption models were obtained with the least sum of the squares of the differences (SSE) between the experimental data and fitted data using nonlinear regressive analysis method.

2.6. Desorption study

The certain amount of adsorbent which was used for the biosorption of $50\,mg\,L^{-1}$ of MO at pH 3.00 was separated from dye solution by filtrating, respectively. Then, MO-loaded MWS was washed with distilled water to remove any unabsorbed dye and were dried at 353 K. The above materials were desorbed by immersed in distilled water, hot water, acid, $0.1\,mol\,L^{-1}$ NaOH, $0.1\,mol\,L^{-1}$ NaCl, $0.1\,mol\,L^{-1}$ Na_2SO_4, $0.1\,mol\,L^{-1}$ sodium dodecyl sulfate (SDS), alcohol, or 10 min of microwave irradiation, respectively. Comparison of these methods was in order to select optimized condition for desorption. In this study, three cycles of biosorption/desorption were performed by using optimized desorption agent.

3. Results and discussion

3.1. Chemical composition and FTIR analysis of NWS and MWS

The percentages of element are 0.226% N, 42.34% C, and 5.81% H for NWS and 0.442% N, 46.32% C, and 6.49% H for MWS, respectively. Elemental sulfur was not detected in NWS and MWS. The increased percentages of C, H, and N about MWS were from CTAB biosorption, calculated from nitrogen content as 54.6 CTAB $mg\,g^{-1}$ onto NWS surface. There are some inorganic elements confirmed by the XRF analysis, such as Si, K, Ca, Fe, Mg, Al, etc. The element Br was detected as 2.75% for MWS by XRF, while Br was not detected for NWS.

Fourier transform infrared spectroscopy (FTIR) was useful to examine the surface groups of the adsorbents and to identify some characteristic functional groups. The FTIR spectra of the NWS and MWS are shown in Fig. 2. There were hydroxyl group and carbonyl group on surface of NWS from analysis [36]. Several bands from lignin and hemicellulose can be seen. From Fig. 2, the strong peak observed at $3{,}410\,cm^{-1}$ is attributed to the −OH vibration of Si−OH, −OH, and so on. The band at $2{,}923\,cm^{-1}$ is the characteristic peak of WS corresponding to the presence of CH_3−CO− of lignin. The band at 1,733 and $1{,}606\,cm^{-1}$ is associated with the stretching vibration of −C=O. The peak associated with the stretch vibration in aromatic rings was verified at $1{,}507\,cm^{-1}$. The peak located at $1{,}243\,cm^{-1}$ was due to stretch vibration of C−O in phenols of lignin. The peak observed at $1{,}422\,cm^{-1}$ was assigned to the stretch vibration of C−O of −COOH. The peak at $1{,}370\,cm^{-1}$ may be from the bending vibration of $-CH_3$.

For MWS, the band at $3{,}410\,cm^{-1}$ is broadened, which is attributed to the vibration of $-NH_2$ of CTAB and −OH of lignin. The intensity of the band at $2{,}923\,cm^{-1}$ increased and shoulder peak near $2{,}855\,cm^{-1}$ was slightly resolved due to the increase in the aliphatic carbon content in MWS, while the peak at $1{,}465\,cm^{-1}$ (bending vibration of $-CH_2$) was slightly increased, which in turn was due to the biosorption of CTAB onto WS surface. This showed that quaternary ammonium groups were successfully introduced to the chain backbone after modification.

The results of elemental analysis and FTIR implied that CTAB have adsorbed onto surface of NWS.

3.2. Effect of adsorbent dose

The effect of adsorbent dosage on the biosorption of dye is shown in Fig. 3.

It can be observed from Fig. 3 that the removal rate of dye increases when concentration and volume of dye keep constant, but the dye biosorption capacity decreases. The former is because the number of sorption sites at the adsorbent surface will increase with increase of adsorbent dosage. For the latter, the per g adsorbent was surrounded by less and less dye molecules with increasing in adsorbent dosage, so that the dye molecules were more difficult to combine the active sites on MWS surface. In addition, it may be attributed to saturation of biosorption sites because of particulate interaction such as aggregation. Hence, the test chose $1.00\,g\,L^{-1}$ as the concentration of adsorbent for MO biosorption.

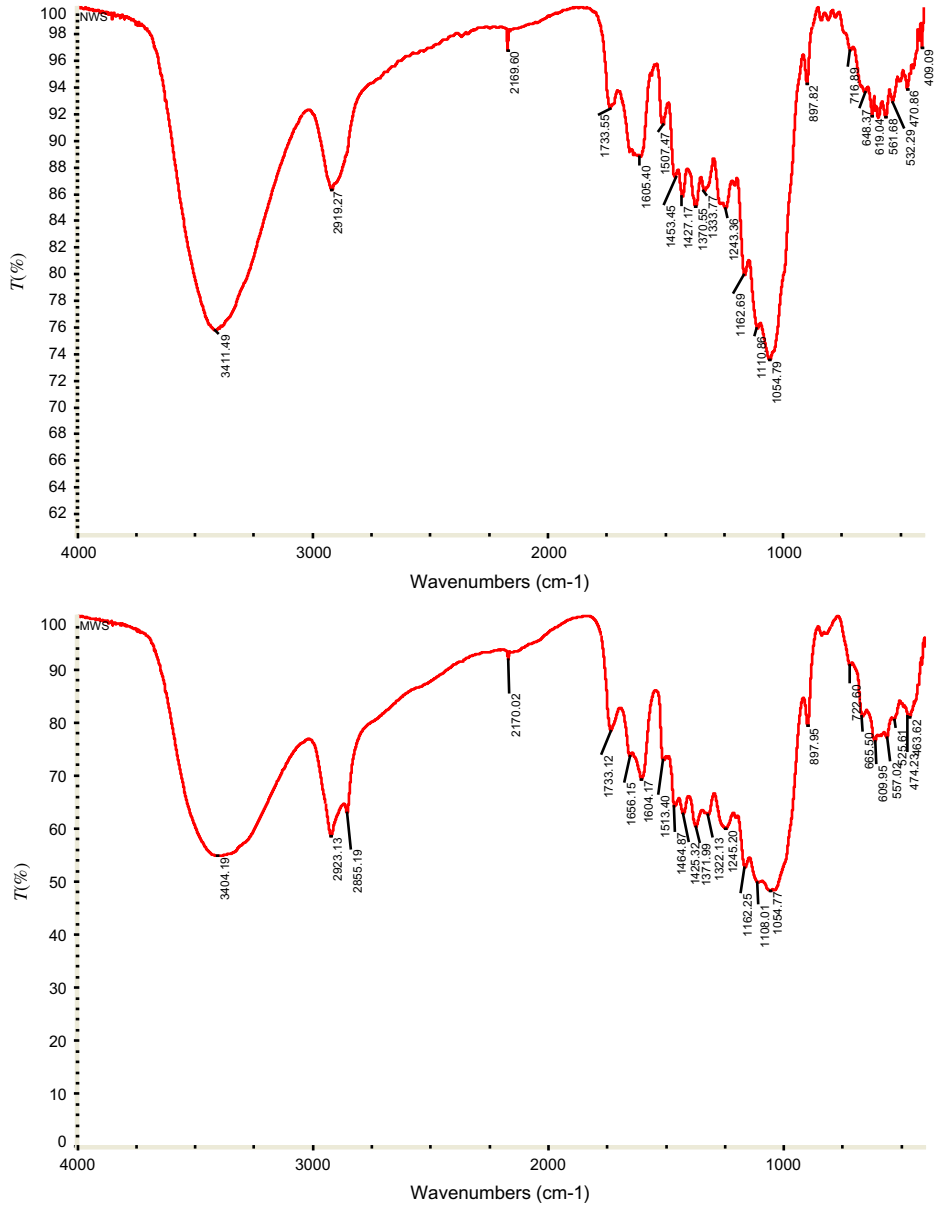

Fig. 2. FTIR spectra of NWS and MWS.

3.3. *Effect of pH on biosorption quantity*

The effect of aqueous solution pH on MO biosorption quantity is shown in Fig. 4, indicating that pH considerably affected the biosorption process of MO.

According to Fig. 4, adsorption was favored at pH 3, while at lower and higher pH values the biosorption capacity decreased. At lower pH values, the concentration of H^+ in the solution was higher. This was formed from $-SO_3^-$ to $-SO_3H$ by binding H^+, which decreased the electrostatic attraction between anionic MO and MWS. That resulted in the decrease in biosorption capacity at lower than pH 3. For higher pH, the drop of biosorption capacity is attributed to the competition between excess OH^- and anionic MO for biosorption sites, so no exchangeable anions will remain on the substrate in this way. In addition, the other possible reason is that pH over the pH_{pzc} make the negative charge at adsorbent surface, which decrease the electrostatic attraction of adsorbent–adsorbate. However, there is still existence of higher biosorption capacity at higher pH value and this showed that the intermolecular interaction such as π–π dispersive interactions between aromatic rings, –N=N– groups of the dye molecule also contribute to the biosorption [37]. Hence, pH of MO solution was adjusted to 3 during next experiments.

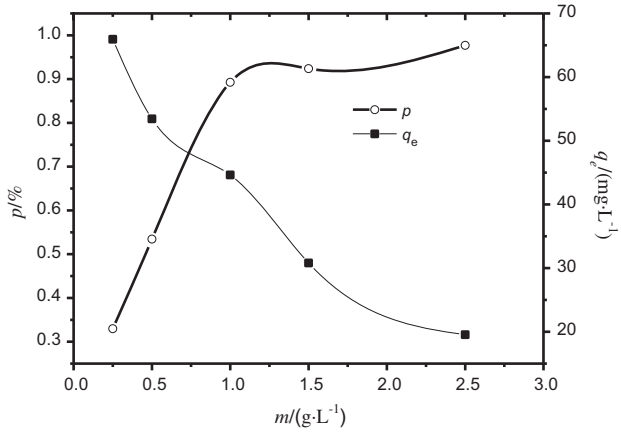

Fig. 3. Effect of MWS dosage on percent removal and biosorption capacity of MO ($C_0 = 30\,mg\,L^{-1}$, pH = 4, contact time 600 min, $T = 303\,K$).

3.4. Effect of salt concentration on biosorption quantity

In practical application, there are commonly certain concentration salt ions in the wastewater. Hence, it is relatively necessary to evaluate the effect of salt on biosorption capacity. Fig. 5 shows effect of NaCl and $CaCl_2$ concentration.

From Fig. 5, it can be seen that when salt concentration increased from 0.00 to $0.05\,mol\,L^{-1}$, the biosorption capacity appeared steep ascending trend, meaning the increase in salt concentration stimulated significantly the biosorption process. When salt concentration above $0.05\,mol\,L^{-1}$, the change trend was stable and hardly alter. This may be attributed to the fact that the presence of salt reduce the thickness of double electrode layer on adsorbent surface, which make it easy the diffusion of dye forward MWS. This contributes to form stronger electrostatic attraction between dye molecular and adsorbent, thus biosorption capacity of MO will increase. Hence, the presence of NaCl and $CaCl_2$ improves the biosorption capacity of MO onto MWS, proving that MWS is able to apply to the wastewater treatment with salt existed.

3.5. Effect of MO concentration in different temperature and equilibrium modeling

The effect of initial concentration on the dye biosorption onto MWS at different temperature was shown in Fig. 5. The biosorption of dye reached equilibrium when the initial concentration increased. For the reason, at first, the interaction between dye and MWS increases gradually with the increasing of the initial concentration. And high concentration dye can drive the dye molecules to combine with the adsorbent. Finally, the biosorption capacity becomes the constant due to the saturation of sorption sites. The increasing temperature results in the decreasing of equilibrium biosorption capacity. That indicates the biosorption process may be exothermal.

The fitted curves of three isotherm sorption models of MWS-MO were also shown as Fig. 6. Parameters of biosorption models and errors were shown in Table 1.

First, it was found that the correlation coefficients and error values of Langmuir are all not practicable. K_F from Freundlich model decreased with the temperature increasing, which indicated the decrease in dye–adsorbent interaction at higher temperature. Value of $1/n$ lay in between 0.1 and 0.5, indicating the favorable biosorption of MO onto MWS. In addition,

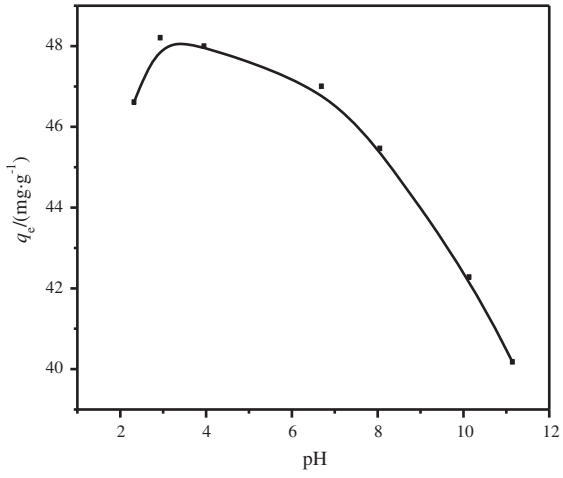

Fig. 4. Effect of pH on biosorption capacity of MO on MWS ($C_0 = 30\,mg\,L^{-1}$, MWS dosage $1.00\,g\,L^{-1}$, contact time 600 min, $T = 303\,K$).

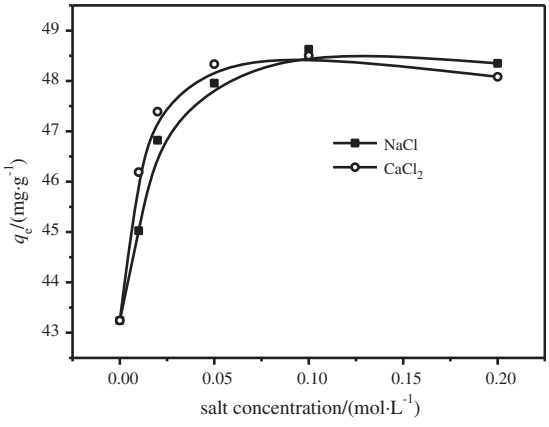

Fig. 5. Effect of salt on biosorption capacity of MO on MWS ($C_0 = 30\,mg\,L^{-1}$, MWS dosage $1.00\,g\,L^{-1}$, contact time 600 min, $T = 303\,K$).

the correlation coefficients and error values of Freundlich model were favorable. These revealed that the data were fitted by Freundlich model better than Langmuir model. In Temkin model, the A and B gradually decreased with the temperature increasing. The R^2 values were close to 1 and error values were lower, suggesting that the Temkin model also fit to depict the biosorption process.

In a word, the Freundlich model can be successful in depicting the biosorption process of MO onto MWS, which suggests that the multilayer coverage of the surface of MWS by MO molecules as well as the heterogeneous biosorption processes. The Temkin and Freundlich models are better to depict the experimental equilibrium biosorption.

Generally speaking, the q_m (obtained from the Langmuir constant) can describe the biosorption capacity of one adsorbent to some extent. Hence, some other adsorbent quantity about MO were listed in Table 2 in order to show the application prospect of MWS (from this study). The value of q_m of MO onto MWS is relatively higher compared with some materials listed in Table 2, while lower than the slightly expensive adsorbents such as carbon coated monolith. In addition, the biosorption condition of MWS–MO is accessible and preparation of MWS is simple, which indicate MWS is an efficient, competitive and promising adsorbent for MO dye.

3.6. Effect of contact time and kinetic modeling

Fig. 7 represents the effects of contact time and temperature on the biosorption capacity of MWS for 30 mg L^{-1} MO. It may be seen that the biosorption capacity increased with longer and longer contact time

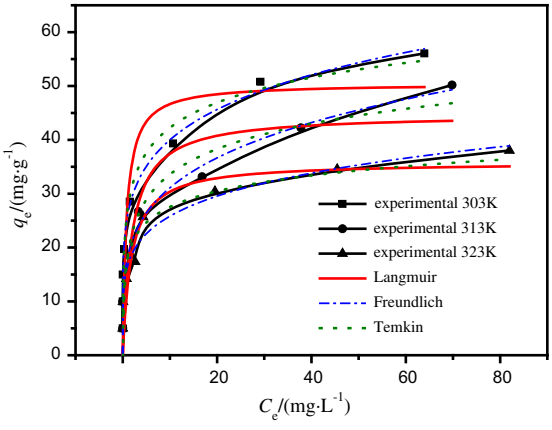

Fig. 6. Biosorption isotherms and the nonlinear fitted curves of three isotherm models at different temperature (MWS dosage 1.00 g L^{-1}, pH = 3).

Table 1
Parameters of biosorption isotherm models and errors at different temperature

T/K	303	313	323
Langmuir			
$q_{m(\text{theo})}$ (mg g^{-1})	50.4	44.8	35.8
K_L (L mg^{-1})	1.22	0.510	0.557
R^2	0.797	0.852	0.864
$q_{e(\text{exp})}$ (mg g^{-1})	56.1	50.2	38.0
SSE	511	261	138
Frendlich			
K_F	25.8	18.0	16.5
$1/n$	0.190	0.237	0.195
R^2	0.994	0.984	0.964
SSE	5.89	14.4	25.2
Temkin			
A	26.7	17.9	17.8
B	6.73	6.81	4.21
R^2	0.990	0.980	0.968
SSE	17.7	37.6	44.0

Note: $SSE = \sum_{i=1}^{n}(q_c - q_e)_i^2$, n is number of experimental points.

until equilibrium. It was evident from the Fig. 7 that the lower temperature is, the faster biosorption is. Hence, high temperature is not beneficial for biosorption. The equilibrium time of MO onto MWS was 520 min. The biosorption kinetics was investigated for better understanding of reaction pathways and dye uptake rate [42]. The plots of the nonlinear forms of four kinetic models for the biosorption of MO on MWS were shown in Fig. 8. The calculated related parameters results were given in Table 3. For the nonlinear fit in 303 K, the coefficients of determination (R^2) for the Elovich and intraparticle diffusion equation were greater than 0.904 and the error values were low, confirming these two models agreed very well with the experimental data. Pseudo-second-order kinetic equation is suitable for describing the biosorption process due to values of R^2 and SSE listed in Table 3.

For the nonlinear fit in different temperature (303, 313, and 323 K; Table 3), the values of R^2 obtained from the pseudo-second-order and Elovich are higher than other two models, while the error values are lower. That is to say, increasing on temperature may increase the moving rate of the adsorbate molecules and Br^- (from CTAB), which might result in more ion exchange between anionic dye and Br^-. That makes biosorption closer to the Elovich.

This suggests that biosorption system be followed by pseudo-second-order and intraparticle diffusion model at normal temperature, based on the assump-

Table 2
MO sorption capacity by other materials: q_m obtained from the Langmuir constant

Adsorbent	q_m (mg g^{-1})	Conditions	References
Bottom ash	16.7	303 K, 4 h	[31]
De-oiled soya	3.62	303 K, 2.5 h	[31]
Coal powder	18.5	303 K, 3 h	[38]
Iron oxide-coated zeolite	3.00	303 K	[39]
Volcanic mud	333	303 K	[40]
Carbon nanotubes	51.8	298 K	[41]
Banana peel	21.0	303 K, 24 h	[42]
Orange peel	20.5	303 K, 24 h	[42]
Carbon coated monolith	102	303 K	[43]
Chromium–benzenedicarboxylates	194	298 K	[44]
Chitoson	9.9	306 K	[45]
Bentonite	33.8	298 K, 10 h	[46]
MWS	50.4	303 K, 8 h	Present study

tion that rate-limiting step may be film diffusion and intraparticle diffusion and the biosorption process is controlled by chemisorption. While at higher temperature, the biosorption of MWS onto MO seems to be more ion exchange described by Elovich.

3.7. Thermodynamic parameters

Thermodynamic studies were performed to find the nature of biosorption process. Thermodynamics parameters Gibbs free energy (ΔG^o), enthalpy (ΔH^o), and entropy (ΔS^o) were calculated by van't Hoff and Gibb's–Helmholtz equations [47]:

$$K_C = \frac{C_{ad,e}}{C_e} \tag{10}$$

$$\Delta G = -RT \ln K_c \tag{11}$$

$$\Delta G^\circ = \Delta H^\circ - T\Delta S^\circ \tag{12}$$

where $C_{ad,e}$ and C_e are the equilibrium concentration of dye (mg g^{-1}) on the adsorbent and solution, respectively. K_c is the equilibrium constant, and the value of K_c in the lowest experimental dye concentration can be obtained. T is the solution temperature (K) and R is the gas constant.

Thermodynamic parameters obtained are given in Table 4.

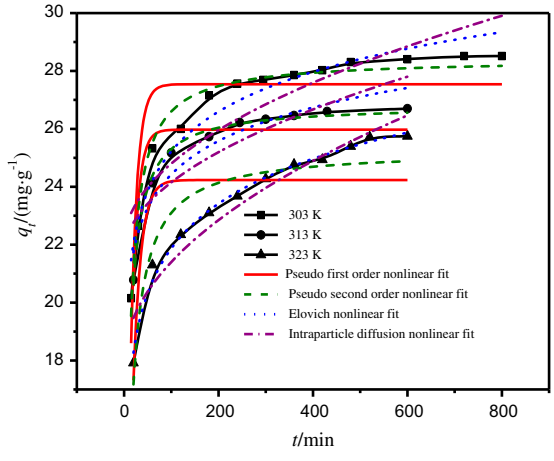

Fig. 7. Effect of contact time on biosorption quantity at different temperature ($C_0 = 30$ mg L^{-1}, MWS dosage1.00 g L^{-1}, pH = 3).

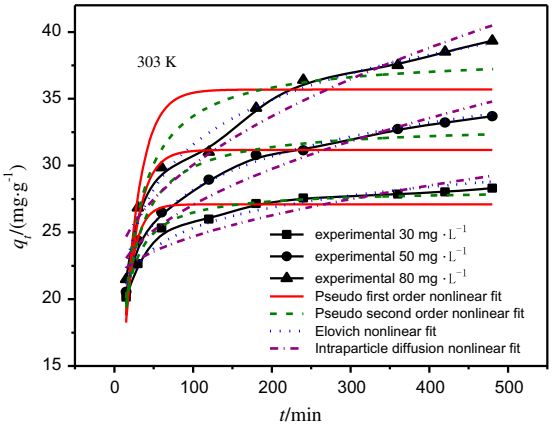

Fig. 8. The fitted curves of four kinetic models at 303 K (MWS dosage 1.00 g L^{-1}, pH = 3).

Table 3
Kinetic parameters for the biosorption of MO onto MWS at different conditions

Kinetic model	T/K				
	303			313	323
C_0 (mg L^{-1})	30	50	80	30	30
Pseudo-first-order					
k_1/(min^{-1})	0.0790	0.0587	0.0498	0.0785	0.0627
q_e/(mg g^{-1})	27.1	31.2	35.7	26.0	24.2
R^2	0.806	0.754	0.749	0.903	0.803
SSE	12.1	39.4	72.2	4.64	17.7
Pseudo-second-order					
$k_2 \times 10^{-3}$ (g mg^{-1} min^{-1})	5.41	2.85	1.92	6.21	4.19
$q_{e(theo)}$ (mg g^{-1})	28.2	33.1	38.3	26.8	25.3
R^2	0.977	0.940	0.917	0.996	0.946
SSE	1.42	9.62	23.9	0.200	5.30
Elovich					
Λ (mg g^{-1} min^{-1})	2007	83.4	32.4	37,434	394
β (g mg^{-1})	0.451	0.275	0.206	0.599	0.447
R^2	0.974	0.996	0.991	0.947	0.994
SSE	3.24	1.27	5.11	2.60	0.555
Intraparticle diffusion					
K_t	0.382	0.650	0.877	0.252	0.350
C	20.9	20.6	21.3	21.6	17.9
R^2	0.904	0.958	0.965	0.836	0.955
SSE	11.4	13.1	20.0	7.60	4.39

As shown in the table, the negative ΔG^o values at different temperatures revealed the spontaneity and feasibility of the biosorption process. The negative ΔH^o values confirmed the exothermic biosorption process. The positive values of ΔS^o which was very small suggested the hardly change randomness at the solid–solution interface during the biosorption of the dye onto MWS. The decrease in the value of the free energy with increase in the temperature indicated that biosorption was favored more at the lower temperature.

3.8. Desorption study

Regeneration and recovery of adsorbents is extremely necessary either for exploring the mechanism or for economic perspective [48–50]. If the dye attached to adsorbent can be desorbed by water, it may be possible that the attachment of the dye onto the adsorbent is through weak bonds. If the acid or alkali can desorb the dye, it may be possible that the attachment of the dye onto the adsorbent is through ion exchange or electrostatic attraction. If organic solvents, such as alcohol, can desorb the dye, it may be possible that the biosorption of the dye onto the adsorbent is through chemisorption.

The regeneration efficiency was investigated and was shown in Fig. 9.

Based on the previous result, the higher pH were disadvantage of biosorption, but beneficial factor for desorption. The best candidate solvent to desorb MO was 60°C hot water according to Fig. 9, which was attributed to the previous study about temperature that high temperature is unbeneficial to biosorption but contributed to desorption. This demonstrated that physical sorption dominated the biosorption process. The organic solvent (alcohol) showed low regeneration efficiency, suggesting the undominant of chemistry biosorption in sorption mechanism. In addition,

Table 4
Thermodynamic parameters for MO biosorption onto MWS

T (K)	293	303	313
ΔG (kJ mol^{-1})	–8.87	–9.21	–9.51
ΔH (kJ mol^{-1})		–0.499	
ΔS (J mol^{-1} K^{-1})		32	

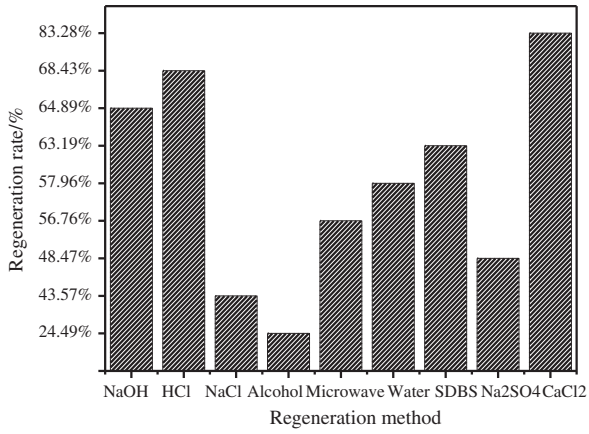

Fig. 9. Comparison of regeneration of MWS.

the desorption method of hot water was economically feasible and makes it possible large-scale promotion of MWS. The 86.7% regeneration efficiency of alcohol also showed chemistry sorption may occupy certain percentage in biosorption mechanism.

4. Conclusion

Biosorption property of MWS toward MO was studied in batch mode. It was favor of biosorption at solution pH 3.0. The high temperature was not beneficial for biosorption, while the salt can improve the biosorption capacity of MO onto MWS. The Freundlich model fitted the equilibrium data well. This suggested that the biosorption reaction might be multilayer and heterogeneous physical biosorption. The kinetic process of MO biosorption onto MWS can be predicted well by Elovich, pseudo-second-order and intraparticle diffusion model. The result confirmed the biosorption process mainly consists of film diffusion and intraparticle diffusion. Furthermore, this also revealed the process involved chemsorption. In addition, the thermodynamics parameters indicated the biosorption process was spontaneous and exothermal. Finally, the desorption study indicated the heat water is better with 83.28% regeneration efficiency. This method is easy and feasible. Therefore, it may be concluded that the MWS is a efficient, environmental, economically feasible alternative, and promising agriculture absorbent for dye from industrial wastewater.

Acknowledgments

This work was funded by the National Natural Science Foundation of China (J1210060). I give my thanks to editor and reviewers for suggestion to improve the quality of this manuscript.

References

[1] T. Robinson, G. McMullan, R. Marchant, P. Nigam, Remediation of dyes in textile effluent: A critical review on current treatment technologies with a proposed alternative, Bioresour. Technol. 77 (2001) 247–255.
[2] E. Bulut, M. Ozacar, A. Sengil, Equilibrium and kinetic data and process design for adsorption of Congo Red onto bentonite, J. Hazard. Mater. 154 (2008) 613–622.
[3] K. Swaminathan, S. Sandhya, A. Carmalin Sophia, K. Pachhade, Y.V. Subrahmanyam, Decolorization and degradation of H-acid and other dyes using ferrous-hydrogen peroxide system, Chemosphere 50 (2003) 619–625.
[4] M. Muthukumar, N. Selvakumar, Studies on the effect of inorganic salts on decoloration of acid dye effluents by ozonation, Dyes Pigm. 62 (2004) 221–228.
[5] A. Alinsafi, M. Khemis, M.N. Pons, J.P. Leclerc, A. Yaacoubi, A. Benhammou, A. Nejmeddine, Electro-coagulation of reactive textile dyes and textile wastewater, Chem. Eng. Process. 44 (2005) 461–470.
[6] A.S. Özcan, A. Özcan, Adsorption of acid dyes from aqueous solutions onto acid activated bentonite, J. Colloid Interf. Sci. 276 (2004) 39–46.
[7] M. Ghaedi, H. Tavallali, M. Sharifi, S.N. Kokhdan, A. Asghari, Preparation of low cost activated carbon from Myrtus communis and pomegranate and their efficient application for removal of Congo red from aqueous solution, Spectrochim. Acta A 86 (2012) 107–114.
[8] A. Mittal, R. Jain, J. Mittal, M. Shrivastava, Adsorptive removal of hazardous dye quinoline yellow from wastewater using coconut-husk as potential adsorbent, Fresenius Environ. Bull. 19 (2010) 1–9.
[9] A. Mittal, V. Thakur, V. Gajbe, Evaluation of adsorption characteristics of an anionic azo dye Brilliant Yellow onto hen feathers in aqueous solutions, Environ. Sci. Pollut. Res. 19 (2012) 2438–2447.
[10] X.F. Ren, X.N. Zhang, L.J. Zhang, R.P. Han, Biosorption of methylene blue by natural and chemical modified wheat straw in fixed-bed column, Desalin. Water Treat. in press, doi: 10.1080/19443994.2012.741776.
[11] A. Mittal, D. Jhare, J. Mittal, Adsorption of hazardous dye eosin yellow from aqueous solution onto waste material de-oiled soya: Isotherm, kinetics and bulk removal, J. Mol. Liq. 179 (2013) 133–140.
[12] R.P. Han, D.D. Ding, Y.F. Xu, W.H. Zou, Y.F. Wang, Y.F. Li, L.N. Zou, Use of rice husk for the adsorption of congo red from aqueous solution in column mode, Bioresour. Technol. 99 (2008) 2938–2946.
[13] A. Mittal, R. Jain, J. Mittal, S. Sikarwar, Removal of yellow ME 7 GL from industrial effluent using electrochemical and adsorption techniques, Int. J. Environ. Pollut. 43 (2010) 308–323.
[14] R.P. Han, P. Han, Z.H. Cai, Z.H. Zhao, M.S. Tang, Kinetics and isotherms of neutral red adsorption on peanut husk, J. Environ. Sci. 20 (2008) 1035–1041.
[15] Y. Safa, H.N. Bhatti, Kinetic and thermodynamic modeling for the removal of direct red-31 and direct orange-26 dyes from aqueous solutions by rice husk, Desalination 272 (2011) 313–322.
[16] Y.J. Wu, L.J. Zhang, C.L. Gao, J.Y. Ma, X.H. Ma, R.P. Han, Adsorption of copper ions and methylene blue in single and binary system on wheat straw, J. Chem. Eng. Data 54 (2009) 3229–3234.
[17] A. Mittal, V. Thakur, V. Gajbe, Adsorptive removal of toxic azo dye amido black 10B by hen feather, Environ. Sci. Pollut. Res. 20 (2013) 260–269.

[18] A. Mittal, V. Thakur, J. Mittal, H. Vardhan, Process development for the removal of hazardous anionic azo dye Congo red from wastewater by using hen feather as potential adsorbent, Desalin. Water Treat. in press, doi: 10.1080/19443994.2013.785030.
[19] G. Moussavi, R. Khosravi, The removal of cationic dyes from aqueous solutions by adsorption onto pistachio hull waste, Chem. Eng. Res. Des. 89 (2011) 2182–2189.
[20] M. Asgher, H.N. Bhatti, Evaluation of thermodynamics and effect of chemical treatments on sorption potential of citrus waste biomass for removal of anionic dyes from aqueous solutions, Ecol. Eng. 38 (2012) 79–85.
[21] H.N. Bhatti, Y. Safai, Removal of anionic dyes by rice milling waste from synthetic effluents: Equilibrium and thermodynamic studies, Desalin. Water Treat. 48 (2012) 267–277.
[22] V.K. Gupta, A. Mittal, D. Jhare, J. Mittal, Batch and bulk removal of hazardous colouring agent rose Bengal by adsorption techniques using bottom ash as adsorbent, RSC Adv. 2 (2012) 8381–8389.
[23] Y. Tian, M. Wu, X.B. Lin, P. Huang, Y. Huang, Synthesis of magnetic wheat straw for arsenic adsorption, J. Hazard. Mater. 193 (2011) 10–16.
[24] W.X. Zhang, H.J. Li, X.W. Kan, L. Dong, H. Yan, Z.W. Jiang, H. Yang, A.M. Li, R.S. Cheng, Adsorption of anionic dyes from aqueous solutions using chemically modified straw, Bioresour. Technol. 117 (2012) 40–47.
[25] C. Li, H.Z. Chen, Z.H. Li, Adsorptive removal of Cr(VI) by Fe-modified steam exploded wheat straw, Process Biochem. 39 (2004) 541–545.
[26] V.B.H. Dang, H.D. Doan, T. Dang-Vuc, A. Lohi, Equilibrium and kinetics of biosorption of cadmium(II) and copper(II) ions by wheat straw, Bioresour. Technol. 100 (2009) 211–219.
[27] B.C. Oei, S. Ibrahim, S.B. Wang, H.M. Ang, Surfactant modified barley straw for removal of acid and reactive dyes from aqueous solution, Bioresour. Technol. 100 (2009) 4292–4295.
[28] C. Namasivayam, M.V. Sureshkumar, Anionic dye adsorption characteristics of surfactant modified coir pith, a waste lignocellulosic polymer, J. Appl. Polym. Sci. 100 (2006) 1538–1546.
[29] Y. Su, B. Zhao, W. Xiao, R. Han, Adsorption behavior of light green anionic dye using cationic surfactant modified wheat straw in batch and column mode, Environ. Sci. Pollut. Res. in press. doi: 10.1007/s11356-013-1571-7.
[30] S. Ibrahim, S.B. Wang, H.M. Ang, Removal of emulsified oil from oily wastewater using agricultural waste barley straw, Biochem. Eng. J. 49 (2010) 78–83.
[31] A. Mittal, A. Malviya, D. Kaur, J. Mittal, L. Kurup, Studies on the adsorption kinetics and isotherms for the removal and recovery of methyl orange from wastewaters using waste materials, J. Hazard. Mater. 148 (2007) 229–240.
[32] K.Y. Foo, B.H. Hameed, Insights into the modeling of adsorption isotherm systems, Chem. Eng. J. 156 (2010) 2–10.
[33] Y.S. Ho, J.C.Y. Ng, G. McKay, Kinetics of pollutant sorption by biosorbents: Review, Sep. Purif. Method 29 (2000) 189–232.
[34] C.W. Cheung, J.F. Porter, G. Mckay, Sorption kinetics for the removal of copper and zinc from effluents using bone char, Sep. Purif. Technol. 19 (2000) 55–64.
[35] W.J. Weber, Jr., J.C. Morris, Kinetic of adsorption on carbon from solution, J. Sanitary Eng. Div. 89 (1962) 31–59.
[36] R.P. Han, L.J. Zhang, C. Song, M.M. Zhang, H.M. Zhu, L.J. Zhang, Characterization of modified wheat straw, kinetic and equilibrium study about copper ion and methylene blue adsorption in batch mode, Carbohyd. Polym. 79 (2010) 1140–1149.
[37] A. Tabak, N. Baltas, B. Afsin, M. Emirik, B. Caglar, E. Eren, Adsorption of reactive red 120 from aqueous solutions by cetylpyridinium–bentonite, J. Chem. Technol. Biotechnol. 85 (2010) 1199–1207.
[38] Z.N. Liu, A.N. Zhou, G.R. Wang, X.G. Zhao, Adsorption behavior of methyl orange onto modified ultrafine coal powder, Chin. J. Chem. Eng. 17 (2009) 942–948.
[39] L. Zhao, W.H. Zou, L.N. Zou, X.T. He, J.Y. Song, R.P. Han, Adsorption of methylene blue and methyl orange from aqueous solution by iron oxide-coated zeolite in fixed bed column: Predicted curves, Desalin. Water Treat. 22 (2010) 258–264.
[40] A.A. Jalil, S. Triwahyono, S.H. Adam, N.D. Rahim, M.A.A. Aziz, N.H.H. Hairom, N.A.M. Razali, M.A.Z. Abidin, M.K.A. Mohamadiah, Adsorption of methyl orange from aqueous solution onto calcined Lapindo volcanic mud, J. Hazard. Mater. 181 (2010) 755–762.
[41] Y.J. Yao, B. He, F.F. Xu, X.F. Chen, Equilibrium and kinetic studies of methyl orange adsorption on multiwalled carbon nanotubes, Chem. Eng. J. 170 (2011) 82–89.
[42] G. Annadurai, R.S. Juang, D.J. Lee, Use of cellulose-based wastes for adsorption of dyes from aqueous solutions, J. Hazard. Mater. 92 (2002) 263–274.
[43] S. Hosseini, M.A. Khan, M.R. Malekbala, W. Cheah, T.S.Y. Choong, Carbon coated monolith, a mesoporous material for the removal of methyl orange from aqueous phase: Adsorption and desorption studies, Chem. Eng. J. 171 (2011) 1124–1131.
[44] E. Haque, J.E. Lee, I.T. Jang, Y.K. Hwang, J.S. Chang, J. Jegal, S.H. Jhung, Adsorptive removal of methyl orange from aqueous solution with metal-organic frameworks, porous chromium–benzenedicarbonxylates, J. Hazard. Mater. 181 (2010) 535–542.
[45] T.K. Saha, N.C. Bhoumik, S. Karmaker, M.G. Ahmed, H. Ichikawa, Y. Fukumori, Adsorption of methyl orange onto chitosan from aqueous solution, J. Water Res. Protect. 2 (2002) 898–906.
[46] D. Leodopoulos, D. Doulia, K. Gimouhopoulos, T.M. Triantis, Single and simultaneous adsorption of methyl orange and humic acid onto bentonite, Appl. Clay Sci. 70 (2012) 84–90.
[47] C. Namasivayam, K. Ranganathan, Waste Fe(III)/Cr(III) hydroxide as adsorbent for the removal of Cr(VI) from aqueous solution and chromium plating industry wastewater, Environ. Pollut. 82 (1993) 255–261.
[48] C. Namasivayam, N. Muniasamy, K. Gayatri, Removal of dyes from aqueous solutions by cellulosic waste orange peel, Bioresour. Technol. 57 (1996) 37–43.
[49] V.K. Gupta, A. Mittal, A. Malviya, J. Mittal, Adsorption of carmoisine A from wastewater using waste materials – bottom ash and de-oiled soya, J. Colloid Interf. Sci. 355 (2009) 24–33.
[50] R.P. Han, Y. Wang, Q. Sun, L.L. Wang, J.Y. Song, X.T. He, C.C. Dou, Malachite green adsorption onto natural zeolite and reuse by microwave irradiation, J. Hazard. Mater. 175 (2010) 1056–1061.